[19] Inger, G. R., "Specific heat inequality effect in the chemically frozen stagnation point boundary layer," ARS J. **30**, 1028–1029 (1960).

[20] Teare, J. D., Hamerling, P., and Kivel, B., "Theory of the shock front. II. High temperature reaction rates," Res. Note 133, Avco Research Lab., Boston, Mass. (June 1959).

[21] Benson, S. W. and Fueno, T., "The mechanism of atom recombination by consecutive vibrational deactivations," J. Chem. Phys. **36**, 1597–1604 (1962).

[22] Rosner, D. E., "Recent advances in convective heat transfer with dissociation and atom recombination," Jet Propulsion **28**, 445–451 (1958).

[23] Rosner, D. E., "Chemically frozen boundary layers with catalytic surface reaction," J. Aerospace Sci. **26**, 281–286 (1959).

[24] Rosner, D. E., "Boundary conditions for the flow of a multicomponent gas," Jet Propulsion **28**, 555–556 (1958).

[25] Inger, G. R., "An analogy between boundary layer pressure gradient and chemical reaction rate effects," J. Aerospace Sci. **27**, 1028–1029 (1960).

[26] Chung, P. M., "A simplified study of the nonequilibrium Couette and boundary layer flows with air injection," NASA TN D-306 (February 1960).

AUGUST 1963 AIAA JOURNAL VOL. 1, NO. 8

Nonequilibrium Dissociating Flow over a Cusped Body

CHÉNG-TING HSU* AND JOHN E. ANDERSON†
Iowa State University, Ames, Iowa

Exact solutions are obtained for a nonequilibrium dissociating flow of a calorically imperfect, diatomic gas over a cusped body that supports a plane, oblique shock. Numerical examples are presented for N_2 at an altitude of 250,000 ft with M_∞ ranging from 13 to 26, and a shock angle of 80°. Comparison of the results obtained from the models of the simple harmonic oscillator and the Lighthill ideal dissociating gas is made. Variations of the pressure, density, temperature, and degree of dissociation along the streamline are obtained.

Nomenclature

a = sound speed
c_p, c_v = specific heat at constant pressure and volume, respectively
D = dissociation energy per unit mass at 0°K
f = partition function
h = enthalpy
k_r = recombination rate parameter
l_D = $h_1 - h_2$, heat of dissociation per unit mass
M = Mach number
m = gram mass per mole
n,s = natural coordinates, distance normal and along the streamline, respectively
p = pressure
Q = heat added
q = flow speed
R = gas constant, $R_1 = 2R_2$ for diatomic gas
S = specific entropy
T = temperature
T_v = characteristic vibrational temperature
v = $1/\rho$, specific volume
t = time
α = degree of dissociation
β = shock angle
Γ = c_{p_0}/c_{v_0}, ratio of specific heats at frozen condition
θ = streamline angle
μ = chemical potential
ξ,η = shock-oriented coordinates, distance normal and along the shock, respectively
ρ = density
ψ = stream function
$\omega(T)$ = a thermal function, as shown in Eq. (9)

Subscripts

1,2 = for atomic and molecular species, respectively
∞ = freestream values
e = equilibrium values
0 = frozen values
s = values immediately behind the shock

Received by IAS November 5, 1962; revision received June 3, 1963. All of the numerical solutions were carried out by the junior author. The authors are much indebted to Eastman Kodak Company for financing all the computer charges.

* Professor, Department of Aerospace Engineering. Member AIAA.

† Graduate Student, Department of Aerospace Engineering. Associate Member AIAA.

Introduction

FOR hypersonic vehicles traveling in air, the gas temperature behind the shock may be high enough to excite the vibrational modes of a diatomic gas and the chemical reactions between the different species in the gas. Since the shock layer is usually very thin, this high-temperature energy, obtained almost instantaneously behind the shock, is absorbed rather gradually by the gas vibrational excitation and gas dissociation. These gradual processes with a finite rate of vibrational relaxation and chemical reaction cause the phenomenon of thermodynamic nonequilibrium behind the shock.

In order to gain some insight into the physics of the nonequilibrium flow, it is advantageous first to investigate this flow over some simple bodies of the sharp or pointed nose type, such as the cusped body, the wedge, and the cone. It is of basic interest to see how in these cases the simple, classical, supersonic flows are modified due to departure from thermodynamic equilibrium. Sedney[1–3] has studied successfully the problems of nonequilibrium vibrational flow over such bodies. Epstein[4] has treated the problem of nonequilibrium dissociating flow behind a plane, oblique shock (or over a cusped body) by using Lighthill's ideal dissociating gas. Capiaux and Washington[5] recently have treated the problem of nonequilibrium dissociating flow past a wedge by using the method of characteristics and assuming also Lighthill's ideal dissociating gas.

The mechanism of vibrational oscillation for a diatomic gas is quite complicated. For simplicity, the assumption of Lighthill's[6] ideal dissociating gas commonly is used, i.e., to

count only one-half of the total vibrational energy excited. Although the Lighthill assumption is quite reasonable, it would be more valuable to treat the dissociating diatomic gas by a more accurate model and to compare it with the Lighthill gas model.

The purpose of the present analysis is to treat the nonequilibrium dissociating flow by using a calorically imperfect, diatomic gas. Only one type of diatomic gas, such as N_2 or O_2, is considered. It is assumed in this analysis that each gas species is thermally perfect during the dissociation process. For a thermally perfect gas, the caloric equation of state for its internal energy or enthalpy is, in general, a function of temperature[7] only. However, the specific heat for the diatomic species in a constant volume or pressure process is not necessarily constant as in the Lighthill ideal gas. For simplicity, the effects of diffusion, viscosity, and heat conductivity in the flow regime of interest are neglected. It also is assumed that this nonequilibrium dissociating flow is always in vibrational equilibrium‡ so that the comparison with Lighthill's gas model is possible. The present analysis is used to obtain the exact solution of a nonequilibrium dissociating flow over a cusped body that supports a plane, oblique shock. The approach taken here is similar to the one introduced by Sedney[1] for a vibrationally relaxing gas but is different from Epstein's[4] treatment. The simple harmonic oscillator is chosen later for the gas model. This result then is compared to the solution obtained by using the Lighthill ideal dissociating gas. It is shown also that the present analysis may be used to obtain the nonequilibrium dissociating flow over a wedge for a calorically imperfect, diatomic gas.

Equations of Motion

The fundamental equations of motion in a steady, two-dimensional, isoenergetic, and nonequilibrium dissociating flow, using natural coordinates, are as follows:[10]

Continuity

$$\frac{1}{\rho}\frac{\partial \rho}{\partial s} + \frac{1}{q}\frac{\partial q}{\partial s} + \frac{\partial \theta}{\partial n} = 0 \tag{1}$$

Momentum

$$\rho q \frac{\partial q}{\partial s} = -\frac{\partial p}{\partial s} \tag{2}$$

$$\rho q^2 \frac{\partial \theta}{\partial s} = -\frac{\partial p}{\partial n} \tag{3}$$

Energy

$$dh + q\,dq = 0 \tag{4}$$

Second Law

$$T\,dS = dh - \frac{dp}{\rho} - \left[\omega_1(T) - \omega_2(T) + R_2 T \ln\frac{4\alpha^2 p}{1-\alpha^2}\right]d\alpha \tag{5}$$

State

$$p = (1+\alpha)\,\rho\,R_2 T \tag{6}$$

$$h = \alpha\,h_1 + (1-\alpha)\,h_2 \tag{7}$$

Reaction Rate

$$q(\partial\alpha/\partial s) = F(\rho, T, \alpha) \tag{8}$$

‡ It would be more realistic to consider the coupling effect between the vibrational relaxation and chemical reaction. This coupling effect for N_2 and O_2 has been considered by Treanor and Marrone[8] and others, and for the mixture of air it has been considered by Lin and Teare.[9]

where

$$\omega_i(T) = \int c_{p_i} dT - T\int c_{p_i}\frac{dT}{T} + h_i' - S_i' T \tag{9}$$

$$h_i = \int c_{p_i} dT + h_i' \tag{10}$$

and $F(\rho, T, \alpha)$ is a given function for the rate of chemical reaction, and h_i' and S_i' are some constant values at a certain temperature.

Equations (1–8) involve eight unknowns, p, ρ, T, q, θ, h, S, and α. Combining Eqs. (1, 2, 5, and 6), together with some thermodynamic relations for S, one is able to eliminate p and ρ from the equations of motion and obtain the following relation:[10]

$$(M_0^2 - 1)\frac{\partial q}{\partial s} + \left[\frac{1}{1+\alpha} - \frac{l_D}{c_{p_0}T}\right]q\frac{\partial \alpha}{\partial s} - q\frac{\partial \theta}{\partial n} = 0 \tag{11}$$

where $M_0^2 = q^2/(\Gamma p/\rho)$ is the frozen Mach number, and

$$\Gamma = c_{p_0}/c_{v_0} = \frac{(dQ/dT)_{p,\alpha}}{(dQ/dT)_{v,\alpha}} = \frac{\alpha c_{p_1} + (1-\alpha)c_{p_2}}{\alpha c_{v_1} + (1-\alpha)c_{v_2}} \tag{12}$$

$$\left[\frac{1}{1+\alpha} - \frac{l_D}{c_{p_0}T}\right]\frac{\partial \alpha}{\partial s} = \frac{1}{\Gamma p}\frac{\partial p}{\partial s} - \frac{1}{\rho}\frac{\partial \rho}{\partial s}$$

The term $[1/(1+\alpha) - l_D/c_{p_0}T]$ has a very significant

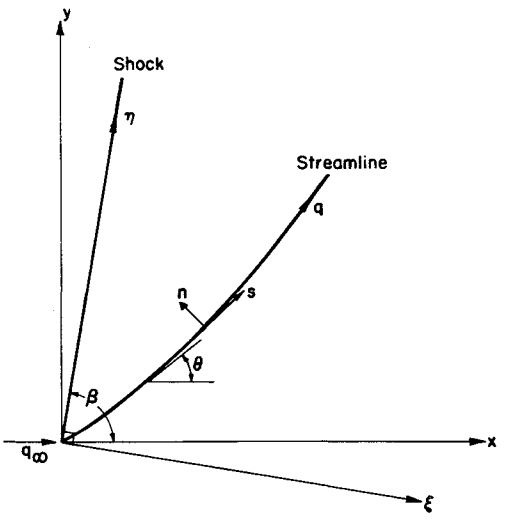

Fig. 1 Streamline in shock-oriented coordinates.

meaning in the determination of the values of streamline curvature and velocity gradient behind a shock.[10] This term would correspond to the general exact expression $[(\partial p/\partial\alpha)_{\rho,S} - (\mu_1 - \mu_2)(\partial p/\partial S)_{\rho,\alpha}/T]/\rho a_0^2$ appearing in the equations of characteristics obtained by Capiaux and Washington[5] provided that each gas species is thermally perfect. This can be shown by comparing Eq. (22) in Ref. 10 directly to Eq. (26) in Ref. 5. In this case the equations of characteristics[5] for nonequilibrium dissociating flow become

$$d\theta \pm \frac{(M_0^2-1)^{1/2}}{\rho q^2}dp - \frac{[1/(1+\alpha) - l_D/c_{p_0}T]}{\rho q}\frac{\partial \alpha}{\partial s}d\psi = 0 \tag{13}$$

For Lighthill's ideal dissociating gas, $l_D = R_2 T + D$ and $c_{p_0} = (4+\alpha)R_2$, one has

$$\frac{1}{1+\alpha} - \frac{l_D}{c_{p_0}T} = \frac{1}{4+\alpha}\left(\frac{3}{1+\alpha} - \frac{D}{R_2 T}\right)$$

which checks with the results used by Capiaux and Washington.[5]

Flow behind an Oblique Shock

For a straight shock, one can see that all the flow variables behind the shock depend only on the distance along the normal to the shock. Therefore, a shock-oriented coordinate system (ξ,η) may be introduced as shown in Fig. 1, and a solution with flow variables independent of η is sought. The relation between the shock-oriented coordinates and the natural coordinates (n,s) is

$$\frac{\partial}{\partial s} = \sin(\beta - \theta)\frac{d}{d\xi} \qquad \frac{\partial}{\partial n} = -\cos(\beta - \theta)\frac{d}{d\xi} \quad (14)$$

since $\partial/\partial\eta = 0$. Substituting Eq. (7) into Eq. (4) and differentiating it with respect to ξ, one has

$$[\alpha c_{p_1} + (1 - \alpha)c_{p_2}]\frac{dT}{d\xi} + l_D\frac{d\alpha}{d\xi} + q\frac{dq}{d\xi} = 0 \quad (15)$$

Equation (11) may be rewritten in shock-oriented coordinates by using Eq. (14):

$$(M_0^2 - 1)\frac{dq}{d\xi} + \left(\frac{1}{1+\alpha} - \frac{l_D}{c_{p_0}T}\right)q\frac{d\alpha}{d\xi} + q\cot(\beta - \theta)\frac{d\theta}{d\xi} = 0 \quad (16)$$

The velocity q can be solved in terms of θ by means of the momentum equations. Combining Eqs. (2) and (3) and using Eq. (14), one can obtain an ordinary differential equation for the velocity relation:

$$dq/d\xi = -q\tan(\beta - \theta)(d\theta/d\xi) \quad (17)$$

This can be integrated easily for a given constant shock angle β and yields

$$q = q_s\cos(\beta - \theta_s)/\cos(\beta - \theta) \quad (18)$$

where q_s and θ_s are known values that can be obtained from the shock relations for a given freestream condition. It may be interesting to note that Eq. (17) can be written as $d[q\cos(\beta - \theta)] = 0$, which indicates that the type of solution presented here could be obtained also by superimposing the solution for a normal shock and a constant velocity parallel to the normal shock.

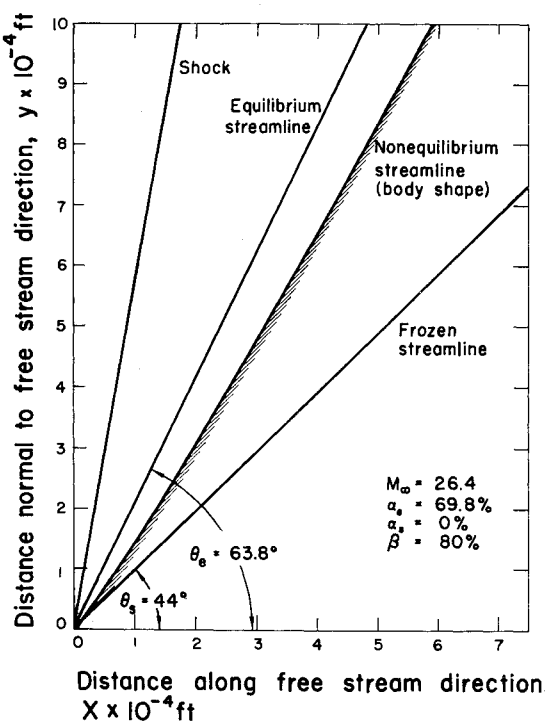

Fig. 2 Body shape supporting an oblique shock for N_2 atmosphere corresponding to 250,000 ft.

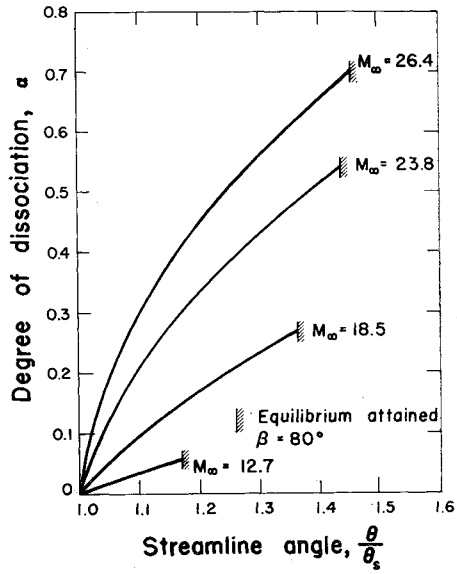

Fig. 3 Degree of dissociation along streamline for N_2 atmosphere corresponding to 250,000 ft.

Now eliminating $d\alpha/d\xi$ from Eqs. (15) and (16) and making use of Eqs. (17) and (18), one obtains the first derivative of T with respect to θ as a function of T, α, and θ:

$$\frac{dT}{d\theta} = -\frac{2(1+\alpha)T}{(1 + \alpha - c_{p_0}T/l_D)\sin 2(\beta - \theta)} + \frac{q_s^2\cos^2(\beta - \theta_s)\tan(\beta - \theta)}{\cos^2(\beta - \theta)} \times \left[\frac{1}{\Gamma R_2(1 + \alpha - c_{p_0}T/l_D)} + \frac{1}{c_{p_0}}\right] \quad (19)$$

Similarly, eliminating $dq/d\xi$ from Eqs. (16) and (17) and

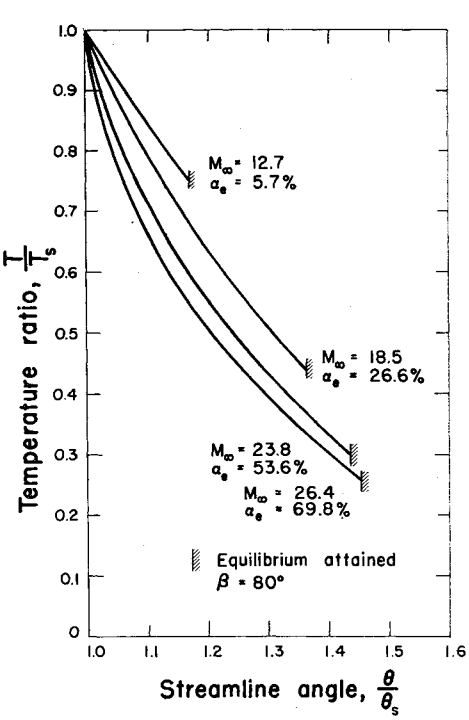

Fig. 4 Temperature distribution along streamline for N_2 atmosphere corresponding to 250,000 ft.

using Eq. (18), the first derivative of α with respect to θ is obtained as a function of T, α, and θ:

$$\left[\frac{l_D}{c_{p_0}T} - \frac{1}{1+\alpha}\right]\frac{d\alpha}{d\theta} = \frac{2}{\sin 2(\beta-\theta)} - \frac{q_s^2\cos^2(\beta-\theta_s)\tan(\beta-\theta)}{(1+\alpha)\Gamma R_2 T\cos^2(\beta-\theta)} \quad (20)$$

Note that c_{p_0} and Γ in Eqs. (19) and (20) are, in general, functions of T and α, and that l_D is a function of T for a calorically imperfect gas. Equations (19) and (20) are two first-order, nonlinear, differential equations in T and α which can be solved in terms of θ by iteration methods.

An explicit solution for ρ may be obtained in terms of θ from Eq. (1) by using Eqs. (14) and (17):

$$\rho/\rho_s = \tan(\beta-\theta_s)/\tan(\beta-\theta) \quad (21)$$

which, upon applying the oblique shock relations, gives

$$\rho/\rho_\infty = \tan\beta/\tan(\beta-\theta) \quad (22)$$

It is interesting to note that the density along any streamline depends only on one freestream condition, ρ_∞.

Furthermore, an expression for p may be obtained from Eq. (3) by making use of Eqs. (14, 18, and 21), giving

$$p = p_s + \rho_s q_s^2 \sin^2(\beta-\theta_s)[1 - \tan(\beta-\theta)/\tan(\beta-\theta_s)] \quad (23)$$

which, with the oblique shock relations, yields

$$p = p_\infty + \rho_\infty q_\infty^2 \sin^2\beta[1 - \tan(\beta-\theta)/\tan\beta] \quad (24)$$

It is necessary also to have a rate equation for the dissociating gas. The rate equation that has been used in the following numerical example is taken from Bloom and Steiger:[11]

$$\frac{d\alpha}{dt} = \frac{\rho}{\rho_d}\left[\frac{k_r(1+\alpha)\rho_d^2}{\bar{m}_1^2}\right]\left[(1-\alpha)e^{-D/R_2T} - \frac{\rho}{\rho_d}\alpha^2\right] \quad (25)$$

where $\rho_d = (\bar{m}_1/2V)(f_1^2/f_2)$; $\bar{m}_1$ is the mass of atom, V the volume, and f the partition function.[6]

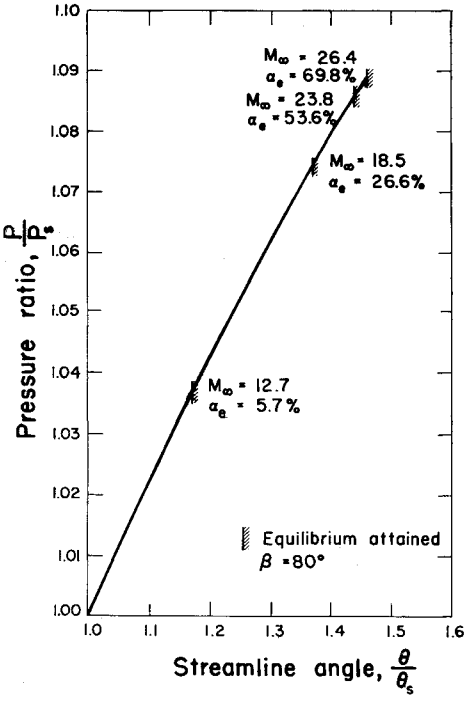

Fig. 5 Pressure distribution along streamline for N_2 atmosphere corresponding to 250,000 ft.

Numerical Solutions

The numerical solutions of Eqs. (19) and (20) yield only the relations between the flow variables (α,T) and the flow inclination θ. In order to express the flow variables as a function of space coordinates (ξ,η), one must be able to relate θ with ξ and η by means of the rate equation (25) and the gradient equation for α, Eq. (20), as given below. First, making use of Eqs. (14) and (18), one has

$$\frac{d\alpha}{dt} = q\frac{d\alpha}{ds} = q_s\cos(\beta-\theta_s)\tan(\beta-\theta)\frac{d\alpha}{d\xi} \quad (26)$$

which, upon integration, yields

$$\xi = q_s\cos(\beta-\theta_s)\int_{\theta_s}^{\theta}\left(\frac{d\alpha/d\theta}{d\alpha/dt}\right)\tan(\beta-\theta)\,d\theta \quad (27)$$

where $d\alpha/d\theta$ and $d\alpha/dt$ are given in Eqs. (20) and (25), respectively. On a streamline, η must be related to ξ as follows:

$$\eta = q_s\cos(\beta-\theta_s)\int_{\theta_s}^{\theta}\left(\frac{d\alpha/d\theta}{d\alpha/dt}\right)d\theta \quad (28)$$

Suppose that all the boundary conditions for the flow variables immediately behind the shock can be determined from the shock relations and the freestream conditions. For each small increment of $\Delta\theta$, one may obtain the corresponding changes of ΔT and $\Delta\alpha$ from Eqs. (19) and (20), respectively, with a digital computer. With the substitution of the new values of ρ, T, and α into Eq. (25), a new reaction rate $d\alpha/dt$ for the corresponding increment of $\Delta\theta$ may be found. Since $d\alpha/dt$ gradually must approach zero as the equilibrium state is attained, the upper limit θ_e of integration in Eqs. (27) and (28) may be determined correspondingly. As $d\alpha/dt \to 0$, $d\alpha/d\theta$ is still finite, and so ξ_e and η_e theoretically become infinite. Actually the curvature of the body approaches zero rather quickly, and the gas is, for all practical purposes, in equilibrium at finite ξ_e and η_e. Performing the integration for ξ and η in Eqs. (27) and (28) for every small increment $\Delta\theta$, one obtains the corresponding space coordinates (ξ,η) for all the flow variables.

Numerical Examples

A few examples were calculated using the ISU Cyclone computer for both N_2 and O_2 atmosphere corresponding to

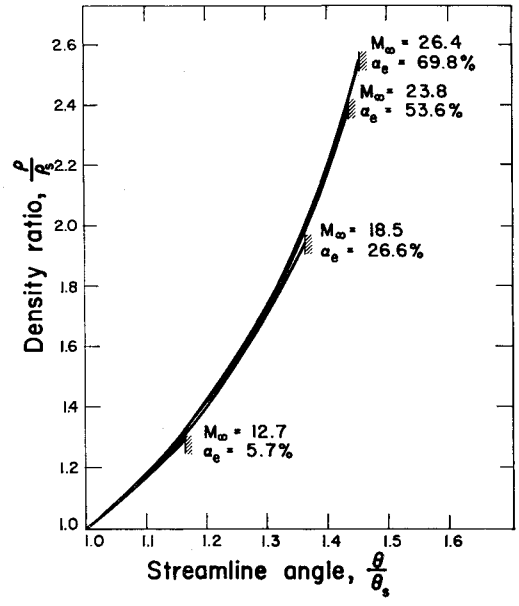

Fig. 6 Density distribution along streamline for N_2 atmosphere corresponding to 250,000 ft.

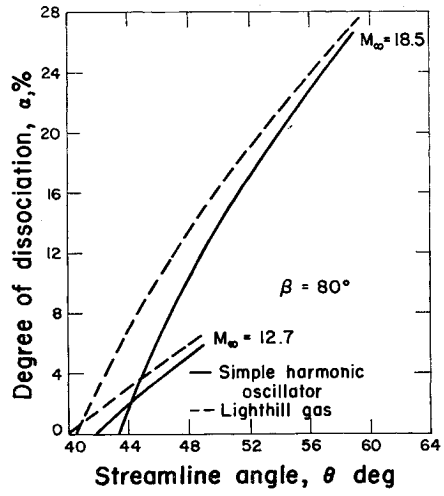

Fig. 7 Comparison of α between the simple harmonic oscillator and Lighthill's ideal gas.

an approximate altitude of 250,000 ft. Some of the results for N_2 are presented below. Two models for the diatomic gas were used in the following examples. One is Lighthill's ideal dissociating gas for which $c_{p_2} = 4R_2$ was used. The other model is the simple harmonic oscillator[7] for which $c_{p_2}/R_2 = (\frac{7}{2}) + [(T_v/2T)/\sinh(T_v/2T)]^2$ was used. Other values used in the rate equation are as follows:[11]

$k_r = 2.5 \times 8.4\ (T/3500°\text{K})^{-2} \times 10^{14}\ (\text{cm}^3/\text{mole})^2/\text{sec}$
$m_1 = 14$ g/mole
$\rho_d = 130$ g/cm^3 (for Lighthill's ideal gas)
$D = 2.95 \times 10^{11}$ ergs/g

The boundary values for the flow variables immediately behind the shock were evaluated at the frozen dissociation condition from the shock relations for a calorically imperfect gas. The shock angle β is taken as 80° for the different freestream velocities; thus, the flow is subsonic behind the shock in all of the cases. One typical streamline is shown in Fig. 2 for N_2 at $M_\infty = 26.4$ or $q_\infty = 25{,}000$ fps. The angle of the streamline changes from the frozen stream angle $\theta_s = 44°$ to equilibrium stream angle $\theta_e = 63.8°$; θ_s corresponds to the wedge angle that would produce the shock if the flow remains frozen ($d\alpha/dt = 0$) behind the shock, and θ_e corresponds to the wedge angle that would produce the shock if the flow attains equilibrium immediately ($d\alpha/dt \to \infty$) behind the shock. In Figs. 3–6, the changes of α, T, p, and ρ along the streamlines by using the simple harmonic oscillator model are plotted for various Mach numbers from 12.7 to 26.4. For all the examples considered, it is interesting to note that the temperature exhibits a large decrease and the density a large increase as the flow approaches equilibrium, whereas the pressure increases rather insignificantly.

A comparison of the results obtained from the models of simple harmonic oscillator and Lighthill's ideal dissociating gas is tabulated in Table 1. The difference in α_e between the two models is significant for low dissociation. For equivalent freestream conditions, the result obtained using the Lighthill model gives about 8.8% higher dissociation than the result of $\alpha_e = 5.7\%$ obtained using the simple harmonic oscillator model. The difference in α_e becomes negligible as the degree of dissociation becomes higher. Comparison of α, T, p, and ρ along streamlines between the two models is shown in Figs. 7–10, respectively. The difference in temperature is most significant in the region immediately behind the shock and then decreases rapidly as the flow approaches equilibrium. It is clear that the vibrational energy, which is the only difference between the two models, accounts for a higher proportion of the total gas energy for low dissociation than for high dissociation. It should be noted that the pressure and density along streamlines are independent of the gas model chosen, as illustrated in Figs. 9 and 10, except that these curves start from different frozen stream angles. This is to be expected, as shown in Eqs. (22) and (24), since p is only a function of θ for a given set of freestream conditions and ρ is only a function of θ for a given ρ_∞. One example has been calculated to compare with Epstein's result using $2D/q_\infty^2 = 2$, $\rho_d/\rho_\infty = 10^6$, $T_\infty = 360°$R, and the rate Eq. (25). For this case, $\alpha_e = 17\%$ as compared to Epstein's case,[4] $\alpha_e = 19\%$.

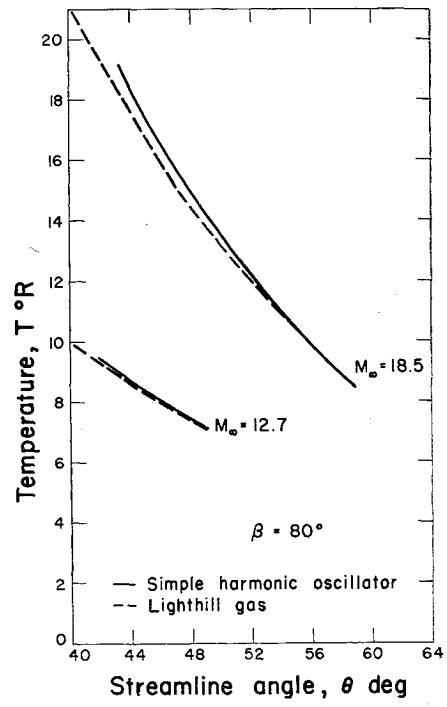

Fig. 8 Comparison of temperature distribution between the simple harmonic oscillator and Lighthill's ideal gas.

Table 1 Results from the models of simple harmonic oscillator and Lighthill's ideal gas for N_2 atmosphere corresponding to 250,000 ft

Gas model	q_∞, fps	p_s, psf	T_s, °R	ρ_s, slugs/ft^3	q_s, fps	θ_s	α_e, %	p_e, psf	T_e, °R	ρ_e, slugs/ft^3	q_e, fps	θ_e
Simple harmonic oscillator	12,000	11.7	9454	6.952×10^{-7}	2652	41.8°	5.7	12.1	7130	9.091×10^{-7}	2435	48.8°
	17,500	24.9	19188	7.327×10^{-7}	3793	42.2°	26.6	26.7	8440	1.425×10^{-6}	3260	58.8°
	22,500	41.3	31157	7.470×10^{-7}	4843	43.8°	53.6	44.8	9334	1.787×10^{-6}	4085	62.8°
	25,000	51.0	38259	7.512×10^{-7}	5369	44.0°	69.8	55.5	9744	1.908×10^{-6}	4530	63.8°
Lighthill's ideal gas	12,000	11.5	9939	6.548×10^{-7}	2716	40.1°	6.2	12.1	7164	9.002×10^{-7}	2417	48.5°
	17,500	24.6	20797	6.655×10^{-7}	3934	40.6°	27.1	26.8	8445	1.418×10^{-6}	3266	58.7°
	22,500	40.6	34182	6.694×10^{-7}	5046	40.7°	53.9	44.8	9304	1.766×10^{-6}	4090	62.6°
	25,000	50.1	42129	6.705×10^{-7}	5603	40.8°	70.1	55.5	9734	1.906×10^{-6}	4525	63.8°

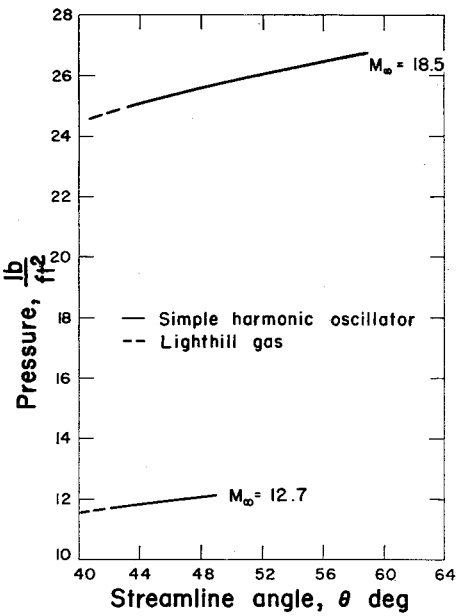

Fig. 9 Comparison of pressure distribution between the simple harmonic oscillator and Lighthill's ideal gas.

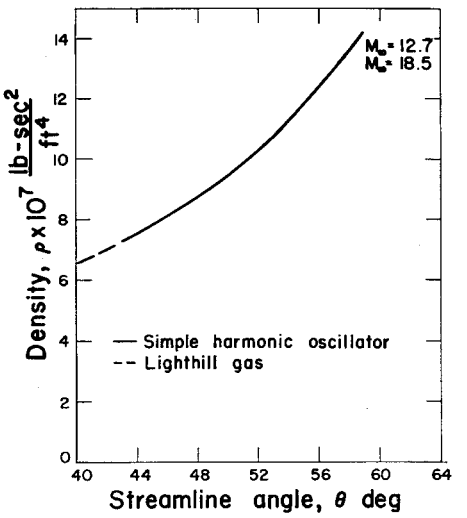

Fig. 10 Comparison of density distribution between the simple harmonic oscillator and Lighthill's ideal gas.

References

[1] Sedney, R., "Some aspects of nonequilibrium flows," J. Aerospace Sci. **28**, 189–196 (1961).

[2] Sedney, R., South, J. C., and Gerber, N., "Characteristics calculation of nonequilibrium flows," Ballistics Research Lab., Aberdeen, Md., BRL Rept. 1173 (1962).

[3] Sedney, R. and Gerber, N., "Nonequilibrium flow over a cone," Inst. Aerospace Sci. Preprint 63-71 (1963).

[4] Epstein, M., "Dissociation relaxation behind a plane, oblique shock wave," J. Aerospace Sci. **28**, 664–665 (1961).

[5] Capiaux, R. and Washington, M., "Nonequilibrium flow past a wedge," AIAA J. **1**, 650–660 (1963).

[6] Lighthill, M. J., "Dynamics of a dissociating gas, Part I, Equilibrium flow," J. Fluid Mech. **2**, 1–32 (1957).

[7] Liepmann, H. W. and Roshko, A., *Elements of Gas Dynamics* (John Wiley and Sons Inc., New York, 1957), Chap. I, p. 37.

[8] Treanor, C. E. and Marrone, P. V., "The effect of dissociation on the rate of vibrational relaxation," Cornell Aeronaut. Lab. CAL Rept. 253-62 (1962).

[9] Lin, S. C. and Teare, J. D., "Rate of ionization behind shock waves in air. II. Theoretical interpretations," Phys. Fluids **6**, 355–375 (1963).

[10] Hsu, C. T., "On the gradient functions for nonequilibrium dissociating flow behind a shock," J. Aerospace Sci. **28**, 337–339 (1961).

[11] Bloom, M. H. and Steiger, M. H., "Inviscid flow with nonequilibrium molecular dissociation for pressure distributions encountered in hypersonic flight," J. Aerospace Sci. **27**, 821–835 (1960).